Research Square

Preprints are preliminary reports that have not undergone peer review.
They should not be considered conclusive, used to inform clinical practice,
or referenced by the media as validated information.

Preclinical Identification of angiotensin II receptor 1 in MEN1 associated pancreatic neuroendocrine neoplasia

Jerena Manoharan
Philipps University of Marburg
Damiano Librizzi
Philipps University of Marburg
Shamim Bagheri
Philipps University of Marburg
Ali Ebrahimifard
Philipps University of Marburg
Jarmila Jedelska
Philipps University of Marburg
Silvia Roth
Philipps University of Marburg
Carmen Bollman
Philipps University of Marburg
Philippe Bertolino
Centre de Recherche en Cancérologie de Lyon
Chang X. Zhang
Centre de Recherche en Cancérologie de Lyon
Sabine Wächter
Philipps University of Marburg
Yuanbiao Tu
China Pharmaceutical University
Katrin Roth
Philipps University of Marburg
Lea Wanke
Philipps University of Marburg
Detlef K. Bartsch
Philipps University of Marburg
Markus Luster
Philipps University of Marburg
Behrooz Yousefi

Philipps University of Marburg

Pietro Di Fazio

difazio@med.uni-marburg.de

Philipps University of Marburg

Research Article

Keywords: MEN1, AT1, pancreatic neuroendocrine neoplasia, radiotracer, BON1, CAM Assay

Posted Date: November 23rd, 2026

DOI: https://doi.org/10.21203/rs.3.rs-11714451/v1

License: This work is licensed under a Creative Commons Attribution 4.0 International License.
Read Full License

Additional Declarations: No competing interests reported.

Abstract

Objective

The angiotensin II receptor type 1 (AT1) is expressed in sporadic pancreatic neuroendocrine neoplasms (pNEN). However, its correlation with multiple endocrine neoplasia 1 (MEN1) remains unknown.

Design

This study focused on the preclinical identification of *MEN1*-associated pNEN via angiotensin II radiotracer ([^{99m}Tc]-HYNIC-PEG4-Ang-II).

Methods

The radiotracer was injected in a blood vessel of the chorio allantoic membrane of chicken that were previously xenografted with human pancreatic neuroendocrine neoplastic cells BON1 and the Mouse Embryo Fibroblasts (MEF). Immunohistochemistry was performed to detect AT1 in CAM xenografts and murine pancreatic tissue

Results

The cells lacking *MEN1* showed a detectable signal by single photon emission computed tomography / computer tomography (SPECT/CT). Instead, the *MEN1* wild type cells were almost negative. Immunohistochemistry evidenced that both the cells carrying *MEN1* and the ones lacking *MEN1* were positive for AT1 and the neuroendocrine marker Chromogranin A (CgA). AT1 was detectable in both *Men1*$^{+/-}$ and *Men1*$^{-/-}$ mice as well. It was significantly stronger in older mice and co-localized with CgA.

Conclusions

Despite the expression of AT1 being independent of *MEN1*, only cells lacking *MEN1* expression could be detectable via the angiotensin II radio tracer. The pre-clinical visualization of *MEN1*-associated pNEN by SPECT/CT of angiotensin II is feasible and could present a potential new diagnostic tool and be implemented for therapy follow-up.

SIGNIFICANCE STATEMENT

The study focused on the expression of the angiotensin 1 receptor 2 in pancreatic neuroendocrine neoplasia. The receptor can be targeted by angiotensin bound to radio tracer thus being able to detect, for the first time, multiple endocrine neoplasia 1 associated neuroendocrine tumors of the pancreas.

This discovery enables the development of new diagnostic tool for those pancreatic neuroendocrine malignancies and provide novel insights for the implementation of therapy follow-up.

INTRODUCTION

Multiple Endocrine Neoplasia Type 1 (MEN1) is a rare autosomal dominant inherited disorder caused by a germline mutation in the MEN1 gene on chromosome 11q13(Manoharan et al. 2017) (Chandrasekharappa et al. 1997)(Brandi et al. 2021).

The diagnosis and treatment of MEN1-associated neuroendocrine tumors have significantly improved in the last decades since the discovery of the causative gene. Particularly with the implementation of regular screening programs, MEN1-associated duodenopancreatic neuroendocrine neoplasms (dpNEN) are diagnosed earlier (starting from 3mm in size) and more frequently through more sensitive imaging techniques such as cross-sectional imaging (endosonography, computed tomography, and magnetic resonance imaging), as well as the introduction of targeted molecular imaging techniques such as [68Ga]Ga-DOTATOC PET/CT (Manoharan et al. 2017; Niederle et al. 2021).

Despite the pivotal role that somatostatin receptor-based imaging diagnostics and therapy play in the management of sporadic neuroendocrine tumors, nearly 30% of patients do not derive benefits (Hofland und Lamberts 2003). This is attributed to certain tumors lacking somatostatin receptor overexpression. Additionally, some patients display an uneven distribution of somatostatin receptors, while others experience receptor downregulation or resistance during treatment (Hofland und Lamberts 2003; Exner et al. 2020). In hereditary diseases like MEN1, the occurrence of multiple and often small dpNEN presents a unique challenge. Retrospective studies showed lower detection rate compared to other imaging methods. Targeting imaging failed to provide additional information (Lastoria et al. 2016; Albers et al. 2017). Instead, targeting imaging was beneficial in case of metastatic disease (Sadowski et al. 2015; Froeling et al. 2012; Albers et al. 2017).

The angiotensin II receptor type 1 (AT1) plays a crucial role in the renin angiotensin system (RAS) and it has been found expressed in all organs (Rodrigues und Bader 2023). It is mainly deputed to promote erythropoiesis (Rodrigues und Bader 2023). Nowadays, it has been found a paracrine secretion of angiotensin II which, in turns, activates AT1. This mechanism could be, in principle, be effective in all tissue and organs of the mammalian body. In particular, it is responsible for regulating the blood pressure, as well as the fat metabolism in the white and brown adipose tissue (Pahlavani et al. 2017). Alteration of the AT1 gene expression characterizes dementia, aging (Tayler et al. 2024) and Alzheimer disease (Ismael et al. 2021). Single nucleotide polymorphisms of AT1 have been detected in patient affected by Parkinson disease (Pierzchlińska et al. 2021). Recently, it has been found that AT1 is implicated in several mechanism responsible for the tumorigenesis in different organs and tissues. It has been observed that AT1 transcription can be promoted by the oncogenic *KRAS*^{G12V} in lung cancer (Volonte et al. 2021). Targeting AT1 by miR-155 inhibits angiogenesis and aggressiveness of glioblastoma (Singh et al. 2020).

Interestingly, previous studies of our research group have shown that AT1 is overexpressed in patients affected by sporadic pNEN as well as *in vitro* in BON1 cells and in the Rip1-Tag2 insulinoma mouse model (Fendrich et al. 2014), (Manoharan et al. 2018), thus showing for the first time the potential of AT1 as biomarker for neuroendocrine tumors. Nonetheless, a further study has identified a strong expression of AT1 in patients affected by small intestine neuroendocrine tumors (Exner et al. 2020)

Recent studies evidenced the possibility to target AT1 for diagnostic purpose. In particular, angiotensin II radiolabelled with technetium ([^{99m}Tc]-HYNIC-PEG4-Ang-II) has shown high specificity for hepatocellular carcinoma cells (Tu et al. 2020a). Instead, the labelling with near infrared fluorescent dye has shown promising results in multiple subcutaneous colorectal cancer xenografts (Zhou et al. 2024).

In order to rapidly prove the potential of AT1 in *MEN1* related pNEN without challenging the dosage of [^{99m}Tc]-HYNIC-PEG4-Ang-II in a mouse model, this study employed the chick chorio allantoic membrane (CAM) assay for xenografting cells lacking the expression of *MEN1* as most suitable model for *MEN1*-associated pNEN. CAM assay has been recently re-discovered as a valuable *in vivo* model for studying the efficacy of anti-cancer substances and molecular mechanisms(Nipper et al. 2024)(Ranjan et al. 2023)(Schneider-Stock und Ribatti 2021)(Menemenli et al. 2024)(Tschanz et al. 2021)(Li et al. 2017) and, recently, it has been increasingly employed as functional model for pre-clinical diagnostic with SPECT or PET based visualization of radio tracers, MRI and fluorescent tracers(Schulze et al. 2023)(Fischer et al. 2012, 2012) (Guder et al. 2022).

Nowadays, many mouse models have been generated in order to study the tumorigenesis of *MEN1*-associated pancreatic neuroendocrine tumors. These models are characterized for the somatic expression of the mutated *Men1*^{tm12qw} or conditional knock out of *Men1* and other genes, which contribute to the tumorigenesis in different organs and pancreas and represent the best suitable model for studying the *MEN1*-associated disease (Fuentes et al. 2024), (Gulde et al. 2022), (Nakano et al. 2020). Interestingly, such models present several limitations concerning the tumor progression and the challenging to get a genetically engineered mouse strain characterized by the alteration of many several genes. Instead, the conditional knock out of the single *Men1* could offer a better model for studying the *MEN1* related pancreas tumorigenesis. The current best representative mouse model of human *MEN1*-associated pNEN is the *Men1* floxed *Rip* Cre, which unfortunately has a too rapid and outgrowing tumor progression (Crabtree et al. 2003).

Alternatively, the *Men1* floxed *Pdx1* Cre mouse model could represent the best option for its slow tumor progression and extremely low adverse effects (Shen et al. 2009). However, the complete loss of *Men1* in homozygouses mice differs them from the human multiple endocrine neoplasia 1, which is characterized by a haploinsufficiency of *MEN1* gene (Brandi et al. 2021). Nonetheless, the complete loss of *Men1* expression in the murine pancreatic cells could better help to understand the dynamic of neuroendocrine tumorigenesis.

Taken together, this study aimed to identify for the first time the expression of AT1 in *MEN1* related pNEN. The cells lacking *MEN1* were xenografted in hen's CAM and further radiolabelled with angiotensin II. The radiotracer was further visualized by SPECT/CT. Furthermore, the expression of AT1 was detected in the pancreatic tissue of young and adult homo- and heterozigouses *Men1* floxed *Pdx1* Cre mice and compared with the neuroendocrine marker chromogranin A (CgA).

MATERIALS and METHODS

Cell culture

Human insulinoma cell line BON1 and the murine embryo fibroblasts MEF *Men1*$^{+/+}$ and *Men1*$^{-/-}$ (Gherardi et al. 2017; Wagener et al. 2022) were grown in DMEM (Gibco, Paisley, UK) supplemented with 10% fetal bovine serum, penicillin (100 Units/ml) and streptomycin (100 µg/ml) at 37° C in a humidified atmosphere containing 5% CO_2. The cells were tested for mycoplasma infection shortly before performing the experiments described below.

Transient knock-down

Based on the previously performed knock down efficiency assay (Wagener et al. 2022), the BON1 cells were transfected for 48h with Hs_MEN1_2 (SI00630238, Qiagen, Hilden Germany) by following the fast transfection protocol suggested by the manufacturer (Qiagen). HiPerfect (Qiagen) was used as transfection reagent and mixed together with the specific siRNAs and serum free medium by following the manufacturer's instructions. A negative transfection control (NTC, Qiagen) was included in all previous experimental settings including the MEN1 knockdown (Wagener et al. 2022).

The Chick Corio Allantoic Membrane (CAM) Assay

The CAM assay was performed in accordance with the EU directive 2010/63/EU for animal experiments and therefore did not require approval by an ethics committee [(2019) Directive 2010/63/EU of the European parliament and of the council of 22 September 2010 on the protection of animals used for scientific purposes. Available online: https://eur-lex.europa.eu/eli/dir/2010/ 63/2019-06-26]. After delivery, the fertilized chicken eggs (Brormann GmbH & Co. KG, Rheda-Wiedenbrück, Germany) were kept at room temperature for at least 2 h. Subsequently, they were cleaned with 70% (v/v) ethanol and incubated at 37.8°C and 60 – 70% humidity in a hatching incubator (Brutmaschine Easy 150, J. Hemel Brutgeräte GmbH, Verl, Germany). After 3 days (embryo development EDD 3), the eggshell was cracked at the broad pole using a manual egg opener. It was carefully removed with the help of forceps, thus obtaining a round window with a diameter of approximately 3 cm. Viable embryos were identified by clear blood vessels and a beating heart (Aleksandrowicz und Herr 2015).

Xenografting of human and murine cells

Xenografting was performed on EDD 8, after the CAM was gently injured using an aseptic lens tissue as previously described (Schulze et al. 2023). A silicon ring was placed directly on the injured area. *MEN1* wild type BON1, *MEN1* knocked down BON1 (48h after siRNA transfection), *Men1*$^{+/+}$ MEFs and *Men1*$^{-/-}$ MEFs. were xenografted. BON-1 cells and MEFs (1×10^6 in 20 µl growth medium) were mixed with 20 µL of Cultrex Basement Membrane Extract (3432-001-01, R&D Systems, Minneapolis MN, USA). The mix of Matrigel and cell suspension (40 µl) was injected into the silicone ring. The round window was covered again with a petri dish. The egg was placed back into the incubator. The vitality of the embryos was examined daily, and tumor growth was observed via stereo microscopy.

Radio labeling

The radiolabeling of HYNIC-PEG4-Ang-II with 99mTechnetium has been established at the Radio pharmacy Section of the Department of Nuclear Medicine of the Philipps University of Marburg by following the previously described procedures (Tu et al. 2020b). 10 µg of HYNIC-PEG-Ang II peptide (approximately 1 mg dissolved in 1 mL saline) was pipetted into a solution made of 100 µL tricine solution (100 mg mL-1 in 25 mM succinate buffer, pH 5.1) and 100 µL of trisodium 3,3□,3□□-phosphintriyltribenzol sulfonate (TPPTS) solution (50 mg mL-1 in 25 mM succinate buffer, pH 5. 1). The solution was decanted into a 10 mL sterile vial. 370–800 MBq $Na^{99m}TcO_4$ (^{99m}Tc eluate) was then added to the vial and the mixture was heated at 100°C for 15 minutes. After cooling at room temperature for 5 minutes, the mixture was diluted with 1 ml of saline and a sample was taken for subsequent quality control measurements by various radio-TLC and HPLC experiments. The radiochemical purity by three radio-TLC procedures using sodium citrate (0.1 M), ammonium acetate (1 M) and methyl ethyl ketone (MEK) was ≥ 98.5% and by isocratic HPLC (32% acetonitril and 2% H_3PO_4) ≥ 92%. The radiolabeling of [^{99m}Tc]-HYNIC-PEG4-Ang II was very high yielding (337–800 MBq) and the solution was used directly for further experiments.

Radio-labeled tracer injection and SPECT/CT

Four days after the injection of the cell suspension, a tumor mass was detectable. The tumor bearing chick embryos were injected with 10 MBq (Mega Becquerel) in a volume of 100 µl of the radiotracer [^{99m}Tc]-HYNIC-PEG4-Ang-II. The radiotracer solution was injected in a peripheral vein of the chorio allantoic membrane by using a 33G needle (Mesoram, PromaMedical GmbH, Munich Germany) and a 1 mL syringe (Schulze et al. 2023). Undesired bleeding caused by the injection can be stopped by applying a cotton swab on the injection site. In case of blood perfusion across the chorio allantoic membrane or nearby the tumor areas, the assay has to be terminated and excluded from the analysis. Embryos are sacrificed after tumor excision.

Single photon emission computed tomography (SPECT/CT) was utilized as imaging modality. The Mediso small animal Nanoscan SPECT/CT (Budapest, Hungary), designed for small animal studies, comprises a SPECT component equipped with a pinhole collimator to achieve high-resolution imaging, along with a CT scanner for attenuation correction.

The SPECT/CT examination protocol involves a three-dimensional measurement of the activity distribution, followed by a CT scan in the transverse plane for morphological imaging. The entire acquisition procedure takes approximately 60 minutes.

Prior to SPECT/CT, the egg was brought back to the incubator for ~30min to ensure the distribution and uptake of the radio labeled tracer. CT scans were performed before each SPECT acquisition.

Analysis of the SPECT/CT images

The reconstructed SPECT and CT images were successfully obtained and co-registered using the Fusion module of PMOD software (ver. 4.305, PMOD Technologies, Ltd., Zurich, Switzerland). This enabled the direct correlation of measured radioactivity with the volume of interest (VOI), facilitating quantitative image analysis. To ensure accurate alignment and prevent misregistration due to SPECT data shifts, an automated protocol was applied for SPECT/CT image matching. Additionally, the alignments were then visually double-checked and verified by a nuclear medicine specialist and biologist (DL, PD). For quantitative analysis of SPECT images, the tumor, background, and total area were manually delineated as Volume of Interest (VOI). The statistical calculations included the Standardized Uptake Value (SUV) and Standard Deviation (SD), derived from the percent injected dose (%ID) per volume (mL).

Statistical analysis was performed using GraphPad Prism (ver. 10.0, GraphPad Software, San Diego, CA, USA) on the SPECT data (P value = 0.0038, **). This involved the application of one-way ANOVA, followed by Turkey's multiple comparisons test, with the objective of comparing the MEN1 wild type BON1, MEN1 knocked down BON1, $Men1^{+/+}$ MEFs and $Men1^{-/-}$ MEFs. series to check the significant differences in the slopes.

Men1 conditional knock out mouse model

The genetically modified *Men1* mouse model was generated by breeding female *Men1*$^{flox/flox}$ ($Men1^{tm1.2Zqw/Flmg}$) with male *Pdx1*$^{Cre/Cre}$ mice. The backcrossing of the heterozygouses *Men1*$^{flox/+}$*Pdx1*$^{Cre/Cre}$ mice was performed to generate *Men1* heterozygouses and homozygouses mice. These mice were characterized for a partial (heterozygous) or complete (homozygous) deletion of the *Men1* gene in the pancreatic tissue. The mice were euthanized and dissected at the age of three, six, nine, twelve and eighteen months old. 12 mice each age group were collected and the dissected pancreatic tissue was fixed in 3.7% formalin (Carl Roth GmbH + Co. KG, Karlsruhe, Germany) and embedded in paraffin. 3 to 6 of FFPE pancreatic tissue have been further processed for the

immunostaining. The animal breeding, housing and euthanasia was conducted according to the animal welfare (ARRIVE Guidelines) and approved by Hesse Animal Committee (G35/2020).

Immunohistochemistry

The tumor, resected from the chick chorioallantoic membrane, and the pancreas dissected from mice (3–6) were formalin fixed and paraffin embedded. 2 µm thin slices were deparaffinized, antigen retrieval was performed with Citrate Buffer (pH 6). After washing, the slices were incubated with 3% H2O2 for 10 minutes and blocked with 10% BSA in PBST. The slices were incubated overnight with 1% BSA (PBST) and the primary antibody against AT1 (1:1000, PAS-20812, Invitrogen) and ChgA (1:1000, NB120-15160, Novus Biologicals). After washing, the slices were incubated for 1 hour with anti-rabbit secondary antibody (diluted in 1% BSA (PBST). After washing the ABC Kit Vectastain (PK-4001, Biozol GmbH, Eching Germany) was added for 1 hour and ImmPACT® DAB Vectastain (SK4105, Biozol) for the final detection. Hematoxylin staining was performed to visualize the nuclei.

Stained Tissue Scan

All the stained tissue slides were scanned by LEICA Aperio AT1 (LEICA, Wetzlar, Germany).

RESULTS

CAM Assay-based detection of the radio-labeled angiotensin tracer

One million of BON1 and mouse embryo fibroblast (MEF) cells were injected on the surface of the CAM at EDD 8. The eggs were divided into 4 groups (6 eggs per group): *MEN1* wild type BON1, *MEN1* knocked down BON1, $Men1^{+/+}$ MEFs and $Men1^{-/-}$ MEFs. The tumor mass derived from all 4 different cells was observable and detectable after 4 days (EDD 12). The eggs, carrying the tumor mass (Table 1), were subjected to the injection of the technetium radio-labeled tracer. 100 µl (10 MBq) of [^{99m}Tc]-HYNIC-PEG4-Ang-II were injected into the peripheral vein of the CAM.

Table 1
Number of CAM xenografts that were injected with the angiotensin II radiotracer ([99mTc]-HYNIC-PEG4-Ang-II). The signal was detected by SPECT/CT. Stable Knock Out (KO). Transient Knock Down (KD) by transfection with siRNA.

BON1	**MEN1 WT**	**MEN1 KO**	**MEN1 KD**
	5	**-**	**4**
MEFs	3	4	-

The eggs were kept at 37°C for 30 minutes before performing the SPECT/CT. The method was able to acquire a detectable signal only in the tumor mass derived from the *MEN1* knocked down BON1 cells (n = 4) and the *Men1*$^{-/-}$ MEFs (n = 4). Instead, the *MEN1* wild type BON1 cells (n = 5) and MEFs (n = 3) evidenced a weak, almost absent signal (Fig. 1 and supplementary Fig. 1–3).

Quantification of the SPECT/CT based detection of the angiotensin II radiotracer

The reconstructed SPECT and CT images were successfully analyzed and co-registered using the Fusion module of PMOD software. The tumor, background, and total area were defined as volumes of interest through manual delineation. As shown in the Fig. 2, the amount of the detected radioactive signal, resulting from the ratio between the radioactivity signal of the xenograft and the radioactivity of the total detected area, was significantly higher (*p = 0.0108) in *MEN1* knocked down BON1 cells (*MEN1*kd) compared to *MEN1* wild type BON1 (*MEN1*wt). The MEFs lacking *Men1* (*Men1*ko) also showed an increase of the signal, although it was not significant if compared with *Men1* wild type MEFs (*Men1*wt), because of the low signal of both *Men1* wild type and knock out cells.

Expression of AT1 in CAM xenograft

In order to confirm the specificity of the binding of the [^{99m}Tc]-HYNIC-PEG4-Ang-II with its associated receptor, the immunohistochemical detection of AT1 has been performed in FFPE tumor xenografts isolated form the CAM assay. As shown in Fig. 3, the xenografts derived from BON1 highlighted a stable expression of AT1, which remained consistent in *MEN1* knocked down BON1 cells too. Interestingly, the xenografts derived from *Men1* depleted MEFs exhibited a stronger expression of AT1 in comparison to *Men1*$^{+/+}$ MEFs. Both BON1 and MEFs were positive for CgA staining, thus evidencing the endocrine origin of the BON1 cells. Unexpectedly, the MEFs showed a CgA positive staining too.

Expression of AT1 in Men1 depleted murine pancreatic tissue

The expression of the angiotensin II receptor 1 was detected in heterozygous (n = 26) and homozygous (n = 24) *Men1*$^{f/f}$ PDX^{CRE} mice (Table 2). As shown in Fig. 4, the expression of AT1 was immunohistochemically detectable in 3 months old mice. AT1 expression was stable in older mice (6 and 9 months) and it increased in 12- and 18-months old mice together with the size of the islets. CgA expression was detected to confirm the neuroendocrine origin of AT1 positive islets. However, AT1 was ubiquitously expressed in the exocrine pancreatic murine tissue too, thus making difficult the visualization of the endocrine AT1. Additionally, young (3 months old) *Men1* wild type mice showed no detectable signal of AT1 thus assuming that its expression correlates inversely with the loss of *Men1*.

Table 2

floxed	Sum	Men1	PDX-Cre	Age (months)	Sex	Median Body Weight (g)
	4	**+/+**	**+/+**	**2,6(2), 10**	**m**	**36.3**
hetero	2	+/-	+/+	3	m	30.66
hetero	1	+/-	+/+	3	f	20.8
hetero	3	+/-	+/+	6	m	28.2
hetero	1	+/-	+/+	6	f	22.3
hetero	3	+/-	+/+	9	m	36.1
hetero	3	+/-	+/+	9	f	31.07
hetero	4	+/-	+/+	12	m	34.55
hetero	2	+/-	+/+	12	f	30.55
hetero	3	+/-	+/+	18	m	38.65
hetero	4	+/-	+/+	18	f	33.01
Homo	4	-/-	+/+	3	m	25.75
Homo	2	-/-	+/+	3	f	22.1
Homo	3	-/-	+/+	6	m	31.7
Homo	3	-/-	+/+	6	f	22.7
Homo	3	-/-	+/+	9	m	31.8
Homo	2	-/-	+/+	9	f	26.15
homo	4	-/-	+/+	12	m	34.25
homo	3	-/-	+/+	12	f	29.8

List of the mice dissected to isolate pancreatic tissue for AT1 and CgA staining. Heteozigous (hetero) and homozygous (homo) for *Men1* gene expression. Sum = 50, m=male, f=female, floxed = 4

Interestingly, AT1 was detected in *Men1*$^{-/-}$ homozygouses mice too. Its expression was notably stronger in those mice, even at three months old age. Here, the loss of *Men1* caused an evident increase of the size and the number of the neuroendocrine islets that would be easily stained for AT1 and CgA. Thus, confirming the results observed in the heterozygouses mice and the inverse correlation between AT1 and *Men1*.

DISCUSSION

The objective of this study was to identify AT1 by technetium radio-labeled angiotensin II for the first time in pre-clinical in vivo model of *MEN1* associated pNEN.

In the last years, various studies have examined the utility of somatostatin-based functional imaging of *MEN1* associated pNENs, yielding unsatisfactory results and severe limitations of such PET/CT-based diagnostic method (Albers et al. 2017) (Sadowski et al. 2015) (Said et al. 2023). In addition to the low benefits but potential superiority of these imaging techniques, the radiation exposure and costs should also be considered. Recently, a study involving 60 *MEN1* patients with over a 6-year follow-up period showed that somatostatin-based PET/CT contributed to a therapy-relevant decision in only 3 out of 26 patients (Said et al. 2023). Additionally, due to radiation exposure, an increased median risk of cancer death of 0.5% was identified during a 6-year observation period (Said et al. 2023). Thus, highlighting the urgent need to find specific markers for *MEN1* associated pNENs.

AT1 has been recently included as oncogene for its ability to promote cancer-related angiogenesis and vascularization (Khan et al. 2023). Its activation, mediated by the binding with angiotensin II, promotes the VEGF pathway, thus leading to the formation of blood vessels useful for the delivery of oxygen and nutrients to the growing tumor mass(Fendrich et al. 2014) (Escobar et al. 2004).

AT1 over expression has been fully described in breast cancer, where it has been indicated as a valid diagnostic marker for identifying a specific sub-population of ER-positive, *ERBB2*-negative patients (Rhodes et al. 2009). Additionally, it could be observed that angiotensin II is responsible for the activation of the VEGF pathway in pancreatic cancer cells by activating AT1 and the extracellular signal-regulated kinase 1/2 (ERK1/2) (Anandanadesan et al. 2008).

Our research group has previously described the overexpression of AT1 in a pancreatic neuroendocrine neoplasia mouse model (RIP1Tag2) (Fendrich et al. 2014). This discovery prompted us to explore AT1 as a promising target for diagnostic and further therapeutic implementation. This investigation gains particular significance in the context of *MEN1*, as patients develop multiple pNENS due to inherited nature.

In the field of neuroendocrine tumors, Exner and colleagues evidenced by autoradiography the expression of *AT1* in human and murine pancreatic and small intestine NEN tissue (Exner et al. 2020). Interestingly, all of these NEN tissues showed a higher level of *AT1* mRNA than those of somatostatin receptor 2 (Exner et al. 2020). Thus, highlighting the possibility to target AT1 via radiolabeled molecular imaging as a new diagnostic tool for pancreatic and small intestine NEN (Exner et al. 2020).

The current study has shown, for the first time, that AT1 is expressed in BON1 and MEF cells lacking *MEN1*. Interestingly, AT1 can be targeted and detected by [^{99m}Tc]-HYNIC-PEG4-Ang-II (SPECT/CT) in vivo, in CAM assay xenografts of those cells lacking *MEN1* expression. Thus supporting, the previous findings carried out with [^{99m}Tc]-HYNIC-PEG4-Ang-II in hepatocellular carcinoma (Tu et al. 2020a).

Immunohistochemical analysis further validated the positive staining for AT1 and CgA in CAM xenografts lacking *MEN1* expression, emphasizing the association of AT1 with *MEN1*-associated neoplastic progression. However, AT1 was detectable in cells carrying a wild type *MEN1*.

Interestingly, the expression of AT1 was observed in both *Men1*$^{+/-}$ and *Men1*$^{-/-}$ mice, with significantly higher expression in older mice. This finding suggests a potential correlation between AT1 expression and the progression of *MEN1*-associated neoplasms. Up to now, no direct correlation has been found between *MEN1* and AT1 and the reason of the binding of angiotensin II in cells lacking *MEN1* has not been clarified yet. One possibility could rely on the epigenetic mechanism modulated by *MEN1*. Previous studies have shown the ability of menin to bind and activate the nuclear Histone-lysine N-methyltransferase 2A (KMT2A) thus promoting acute leukemia (Kühn und Ganser 2024) (Di Fazio 2023). The loss of *MEN1* expression would block the activity of KMT2A and the further transcription of *AT1* gene thus reducing the protein level of AT1. Furthermore, the epigenetic regulation mediated by the miR-155 could inhibit the translation of *AT1*, thus lowering its cellular protein level and explaining the decrease of the binding with angiotensin II (Singh et al. 2020). However, both mechanisms are not able to clarify the mechanism elucidated in this study. The binding of angiotensin II to AT1 could probably rely on post-transcriptional modifications of the receptor itself, e.g. phosphorylation and or ubiquitination (Liu et al. 2019) of certain amino acid residues, which would not affect the expression of AT1 but strongly decrease the binding affinity for angiotensin II. Alternatively, the direct binding of CD74, highly expressed in neuroendocrine tumors (Busse et al. 2020) and pancreatic ductal adenocarcinoma (Zhang et al. 2021), to AT1 could be able to inhibit its translocation at the cellular surface (Szaszák et al. 2008), which in turn causes a reduction of the binding of angiotensin II, as shown in our proposed model. However, no correlation between CD74 and *MEN1*-associated pNEN has been found yet.

The strength of this study is represented by *Men1*-associated murine pNEN. The mouse model represents a valuable tool to explore *MEN1*-associated pNEN tumorigenesis, as these mice develop pancreatic neuroendocrine tumors, in a time frame of 12 months, originating from the islet cells lacking permanently the expression of *Men1*.

Weaknesses of this preclinical study include that, in addition to AT1 expression, the detection of somatostatin receptor was not performed. Therefore, a direct comparison of these receptors is not possible. Furthermore, a SPECT/CT examination of the *Men1* mice could not be conducted, thus limiting the study to the only detection of AT1 in the pancreatic tissue.

In conclusion, this preclinical study proved that AT1 could be targeted in vivo by [^{99m}Tc]-HYNIC-PEG4-Ang-II in human and murine cells lacking *MEN1*, thus representing a strong candidate for targeted imaging in *MEN1* associated pNENs. Furthermore, the correlation between AT1 expression and tumor progression highlights its potential as diagnostic and therapeutic target. Further research is needed to unravel the molecular mechanisms driving the *AT1-MEN1* axis. Future application to test the possibility to synthesize and detect the radio-labeled angiotensin II by PET/CT, e.g. by coupling this protein with

Gallium or Fluorine, could raise AT1 as a novel diagnostic and follow-up tool for *MEN1*-associated pNENs.

Declarations

Conflicts of interest

The authors declare no conflicts.

Ethical approval

The animal breeding, housing and euthanasia was conducted according to the animal welfare (ARRIVE Guidelines) and approved by Hesse Animal Committee (G35/2020).

Funding

The study has been founded by the Habilitation Grant to Jerena Manoharan. The publication costs have been granted by Publikationsfonds from Philipps University of Marburg

Author Contribution

DL and PD performed the SPECT/CT; DL, SR, JJ, CB, KR, and PD performed the CAM assay; SR, SW and PD animal breeding and dissection; SR cell culture and transfection; BY and AE synthesis of the radio tracer; YT synthesis of the angiotensin ligand; KR, LW acquisition and analysis of 3D micrographs; DL, SB, AE and PD analyzed the data and performed the statistical analysis; PB and CXZ concept and design of the animal model; PD design of the work and project coordination; JM, DL and PD wrote the draft; DKB, ML, revised the manuscript.All authors have approved the submitted version and any substantially modified version that involves the author's contribution to the study.All authors have agreed both to be personally accountable for the author's own contributions and to ensure that questions related to the accuracy or integrity of any part of the work, even ones in which the author was not personally involved, are appropriately investigated, resolved, and the resolution documented in the literature.

Acknowledgement

We thank the mouse pathology facility and Frederik Helmprobst for the technical and scientific support. We thank Mareike Meyer of the Institute of Pathology at Philipps University Marburg for the tissue scan assistance. HYNIC-PEG4-Ang-II was a kindly gift of Yuanbiao Tu (State Key Laboratory of Natural Medicine, Department of Biomedical Engineering, School of Engineering, China Pharmaceutical

University, Nanjing, China). We thank Ann-Katrin Mink, Birgit Herbst-Brüch, Eva Rittich and Govi Kotipalli for their valuable assistance.

Data Availability

All data supporting the findings of this study are available within the paper and its Supplementary Information.

References

1. Albers, Max B.; Librizzi, Damiano; Lopez, Caroline L.; Manoharan, Jerena; Apitzsch, Jonas C.; Slater, Emily P. et al. (2017): Limited Value of Ga-68-DOTATOC-PET-CT in Routine Screening of Patients with Multiple Endocrine Neoplasia Type 1. In: *World journal of surgery* 41(6), S. 1521–1527. DOI: 10.1007/s00268-017-3907-9.
2. Aleksandrowicz, Ewa; Herr, Ingrid (2015): Ethical euthanasia and short-term anesthesia of the chick embryo. In: *ALTEX* 32(2), S. 143–147. DOI: 10.14573/altex.1410031.
3. Anandanadesan, Rathai; Gong, Qiaoke; Chipitsyna, Galina; Witkiewicz, Agnes; Yeo, Charles J.; Arafat, Hwyda A. (2008): Angiotensin II induces vascular endothelial growth factor in pancreatic cancer cells through an angiotensin II type 1 receptor and ERK1/2 signaling. In: *Journal of gastrointestinal surgery: official journal of the Society for Surgery of the Alimentary Tract* 12(1), S. 57–66. DOI: 10.1007/s11605-007-0403-9.
4. Brandi, Maria Luisa; Agarwal, Sunita K.; Perrier, Nancy D.; Lines, Kate E.; Valk, Gerlof D.; Thakker, Rajesh V. (2021): Multiple Endocrine Neoplasia Type 1: Latest Insights. In: *Endocrine reviews* 42(2), S. 133–170. DOI: 10.1210/endrev/bnaa031.
5. Busse, Antonia; Mochmann, Liliana H.; Spenke, Christiane; Arsenic, Ruza; Briest, Franziska; Jöhrens, Korinna et al. (2020): Immunoprofiling in Neuroendocrine Neoplasms Unveil Immunosuppressive Microenvironment. In: *Cancers* 12(11). DOI: 10.3390/cancers12113448.
6. Chandrasekharappa, S. C.; Guru, S. C.; Manickam, P.; Olufemi, S. E.; Collins, F. S.; Emmert-Buck, M. R. et al. (1997): Positional cloning of the gene for multiple endocrine neoplasia-type 1. In: *Science (New York, N.Y.)* 276 (5311), S. 404–407. DOI: 10.1126/science.276.5311.404.
7. Crabtree, Judy S.; Scacheri, Peter C.; Ward, Jerrold M.; McNally, Sara R.; Swain, Gary P.; Montagna, Cristina et al. (2003): Of mice and MEN1: Insulinomas in a conditional mouse knockout. In: *Molecular and cellular biology* 23(17), S. 6075–6085. DOI: 10.1128/MCB.23.17.6075-6085.2003.
8. Di Fazio, Pietro (2023): Targeting menin: a promising therapeutic strategy for susceptible acute leukemia subtypes. In: *Signal transduction and targeted therapy* 8(1), S. 384. DOI: 10.1038/s41392-023-01627-w.
9. Escobar, Elizabeth; Rodríguez-Reyna, Tatiana Sofía; Arrieta, Oscar; Sotelo, Julio (2004): Angiotensin II, cell proliferation and angiogenesis regulator: biologic and therapeutic implications in cancer. In: *Current vascular pharmacology* 2(4), S. 385–399. DOI: 10.2174/1570161043385556.

10. Exner, Samantha; Schuldt, Claudia; Sachindra, Sachindra; Du, Jing; Heing-Becker, Isabelle; Licha, Kai et al. (2020): AGTR1 Is Overexpressed in Neuroendocrine Neoplasms, Regulates Secretion and May Potentially Serve as a Target for Molecular Imaging and Therapy. In: *Cancers* 12(11). DOI: 10.3390/cancers12113138.
11. Fendrich, V.; Lopez, C. L.; Manoharan, J.; Maschuw, K.; Wichmann, S.; Baier, A. et al. (2014): Enalapril and ASS inhibit tumor growth in a transgenic mouse model of islet cell tumors. In: *Endocrine-related cancer* 21(5), S. 813–824. DOI: 10.1530/ERC-14-0175.
12. Fischer, Eliane; Grünberg, Jürgen; Cohrs, Susan; Hohn, Alexander; Waldner-Knogler, Karin; Jeger, Simone et al. (2012): L1-CAM-targeted antibody therapy and (177)Lu-radioimmunotherapy of disseminated ovarian cancer. In: *International journal of cancer* 130(11), S. 2715–2721. DOI: 10.1002/ijc.26321.
13. Froeling, Vera; Elgeti, Florian; Maurer, Martin H.; Scheurig-Muenkler, Christian; Beck, Alexander; Kroencke, Thomas J. et al. (2012): Impact of Ga-68 DOTATOC PET/CT on the diagnosis and treatment of patients with multiple endocrine neoplasia. In: *Annals of nuclear medicine* 26(9), S. 738–743. DOI: 10.1007/s12149-012-0634-z.
14. Fuentes, Mary Esmeralda; Lu, Xiaoyin; Flores, Natasha M.; Hausmann, Simone; Mazur, Pawel K. (2024): Combined deletion of MEN1, ATRX and PTEN triggers development of high-grade pancreatic neuroendocrine tumors in mice. In: *Scientific reports* 14(1), S. 8510. DOI: 10.1038/s41598-024-58874-2.
15. Gherardi, Samuele; Ripoche, Doriane; Mikaelian, Ivan; Chanal, Marie; Teinturier, Romain; Goehrig, Delphine et al. (2017): Menin regulates Inhbb expression through an Akt/Ezh2-mediated H3K27 histone modification. In: *Biochimica et biophysica acta*. *Gene regulatory mechanisms* 1860(4), S. 427–437. DOI: 10.1016/j.bbagrm.2017.02.003.
16. Guder, Wiebke K.; Hartmann, Wolfgang; Buhles, Clarissa; Burdack, Maike; Busch, Maike; Dünker, Nicole et al. (2022): 5-ALA-mediated fluorescence of musculoskeletal tumors in a chick chorio-allantoic membrane model: preclinical in vivo qualification analysis as a fluorescence-guided surgery agent in Orthopedic Oncology. In: *Journal of orthopaedic surgery and research* 17(1), S. 34. DOI: 10.1186/s13018-022-02931-x.
17. Gulde, Sebastian; Foscarini, Alessia; April-Monn, Simon L.; Genio, Edoardo; Marangelo, Alessandro; Satam, Swapna et al. (2022): Combined Targeting of Pathogenetic Mechanisms in Pancreatic Neuroendocrine Tumors Elicits Synergistic Antitumor Effects. In: *Cancers* 14(22). DOI: 10.3390/cancers14225481.
18. Hofland, Leo J.; Lamberts, Steven W. J. (2003): The pathophysiological consequences of somatostatin receptor internalization and resistance. In: *Endocrine reviews* 24(1), S. 28–47. DOI: 10.1210/er.2000-0001.
19. Ismael, Saifudeen; Mirzahosseini, Golnoush; Ahmed, Heba A.; Yoo, Arum; Kassan, Modar; Malik, Kafait U.; Ishrat, Tauheed (2021): Renin-Angiotensin System Alterations in the Human Alzheimer's

Disease Brain. In: *Journal of Alzheimer's disease: JAD* 84(4), S. 1473–1484. DOI: 10.3233/JAD-215051.

20. Khan, Nihad Ashraf; Elsori, Deena; Rashid, Gowhar; Tamanna, Sonia; Chakraborty, Ananya; Farooqi, Adeeba et al. (2023): Unraveling the relationship between the renin-angiotensin system and endometrial cancer: a comprehensive review. In: *Frontiers in oncology* 13, S. 1235418. DOI: 10.3389/fonc.2023.1235418.
21. Kühn, Michael W. M.; Ganser, Arnold (2024): The Menin story in acute myeloid leukaemia-The road to success. In: *British journal of haematology*. DOI: 10.1111/bjh.19508.
22. Lastoria, Secondo; Marciello, Francesca; Faggiano, Antongiulio; Aloj, Luigi; Caracò, Corradina; Aurilio, Michela et al. (2016): Role of (68)Ga-DOTATATE PET/CT in patients with multiple endocrine neoplasia type 1 (MEN1). In: *Endocrine* 52(3), S. 488–494. DOI: 10.1007/s12020-015-0702-y.
23. Li, Bo; Qian, Ming; Cao, Hao; Jia, Qi; Wu, Zhipeng; Yang, Xinghai et al. (2017): TGF-β2-induced ANGPTL4 expression promotes tumor progression and osteoclast differentiation in giant cell tumor of bone. In: *Oncotarget* 8(33), S. 54966–54977. DOI: 10.18632/oncotarget.18629.
24. Liu, Chen; Luo, Renna; Wang, Wei; Peng, Zhangzhe; Johnson, Gail V. W.; Kellems, Rodney E.; Xia, Yang (2019): Tissue Transglutaminase-Mediated AT1 Receptor Sensitization Underlies Pro-inflammatory Cytokine LIGHT-Induced Hypertension. In: *American journal of hypertension* 32(5), S. 476–485. DOI: 10.1093/ajh/hpz018.
25. Manoharan, Jerena; Fendrich, Volker; Di Fazio, Pietro; Bollmann, Carmen; Roth, Silvia; Joos, Barbara et al. (2018): Chemoprevention with Enalapril and Aspirin in Men1(+/T) Knockout Mouse Model. In: *Neuroendocrinology* 107(3), S. 257–266. DOI: 10.1159/000492224.
26. Manoharan, Jerena; Raue, Friedhelm; Lopez, Caroline L.; Albers, Max B.; Bollmann, Carmen; Fendrich, Volker et al. (2017): Is Routine Screening of Young Asymptomatic MEN1 Patients Necessary?In: *World journal of surgery* 41(8), S. 2026–2032. DOI: 10.1007/s00268-017-3992-9.
27. Menemenli, Nazlı Şevval; Özcan, Özün; Hüsnügil, H. Hazal; Güleç Taşkıran, Aliye Ezgi; Oral, Göksu; Akyol, Aytekin; Banerjee, Sreeparna (2024): The Chorioallantoic Membrane (CAM) Assay for the Analysis of Starvation-Induced Autophagy. In: *Methods in molecular biology (Clifton, N.J.)*. DOI: 10.1007/7651_2024_562.
28. Nakano, Kenzo; Masui, Toshihiko; Yogo, Akitada; Uchida, Yuichiro; Sato, Asahi; Kasai, Yosuke et al. (2020): Chloroquine induces apoptosis in pancreatic neuroendocrine neoplasms via endoplasmic reticulum stress. In: *Endocrine-related cancer* 27(7), S. 431–439. DOI: 10.1530/ERC-20-0028.
29. Niederle, Bruno; Selberherr, Andreas; Bartsch, Detlef K.; Brandi, Maria L.; Doherty, Gerard M.; Falconi, Massimo et al. (2021): Multiple Endocrine Neoplasia Type 1 and the Pancreas: Diagnosis and Treatment of Functioning and Non-Functioning Pancreatic and Duodenal Neuroendocrine Neoplasia within the MEN1 Syndrome - An International Consensus Statement. In: *Neuroendocrinology* 111(7), S. 609–630. DOI: 10.1159/000511791.
30. Nipper, Allison J.; Warren, Emilie A. K.; Liao, Kershena S.; Liu, Hsuan-Chen; Michikawa, Chieko; Porter, Caroline E. et al. (2024): Chick Embryo Chorioallantoic Membrane as a Platform for Assessing the In

Vivo Efficacy of Chimeric Antigen Receptor T-cell Therapy in Solid Tumors. In: *ImmunoHorizons* 8(8), S. 598–605. DOI: 10.4049/immunohorizons.2400059.

31. Pahlavani, Mandana; Kalupahana, Nishan S.; Ramalingam, Latha; Moustaid-Moussa, Naima (2017): Regulation and Functions of the Renin-Angiotensin System in White and Brown Adipose Tissue. In: *Comprehensive Physiology* 7(4), S. 1137–1150. DOI: 10.1002/cphy.c160031.
32. Pierzchlińska, Anna; Sławek, Jarosław; Mak, Monika; Gawrońska-Szklarz, Barbara; Białecka, Monika (2021): Genetic polymorphisms in the renin-angiotensin system and cognitive decline in Parkinson's disease. In: *Molecular biology reports* 48(7), S. 5541–5548. DOI: 10.1007/s11033-021-06569-6.
33. Ranjan, Raphela A.; Muenzner, Julienne K.; Kunze, Philipp; Geppert, Carol I.; Ruebner, Matthias; Huebner, Hanna et al. (2023): The Chorioallantoic Membrane Xenograft Assay as a Reliable Model for Investigating the Biology of Breast Cancer. In: *Cancers* 15(6). DOI: 10.3390/cancers15061704.
34. Rhodes, Daniel R.; Ateeq, Bushra; Cao, Qi; Tomlins, Scott A.; Mehra, Rohit; Laxman, Bharathi et al. (2009): AGTR1 overexpression defines a subset of breast cancer and confers sensitivity to losartan, an AGTR1 antagonist. In: *Proceedings of the National Academy of Sciences of the United States of America* 106(25), S. 10284–10289. DOI: 10.1073/pnas.0900351106.
35. Rodrigues, André F.; Bader, Michael (2023): The contribution of the AT1 receptor to erythropoiesis. In: *Biochemical pharmacology* 217, S. 115805. DOI: 10.1016/j.bcp.2023.115805.
36. Sadowski, Samira M.; Millo, Corina; Cottle-Delisle, Candice; Merkel, Roxanne; Yang, Lily A.; Herscovitch, Peter et al. (2015): Results of (68)Gallium-DOTATATE PET/CT Scanning in Patients with Multiple Endocrine Neoplasia Type 1. In: *Journal of the American College of Surgeons* 221(2), S. 509–517. DOI: 10.1016/j.jamcollsurg.2015.04.005.
37. Said, Maha; Krogh, Jesper; Feldt-Rasmussen, Ulla; Rasmussen, Åse Krogh; Kristensen, Thomas Skaarup; Rossing, Caroline Maria et al. (2023): Imaging surveillance in multiple endocrine neoplasia type 1: Ten years of experience with somatostatin receptor positron emission tomography. In: *Journal of neuroendocrinology* 35(8), e13322. DOI: 10.1111/jne.13322.
38. Schneider-Stock, Regine; Ribatti, Domenico (2021): The CAM Assay as an Alternative In Vivo Model for Drug Testing. In: *Handbook of experimental pharmacology* 265, S. 303–323. DOI: 10.1007/164_2020_375.
39. Schulze, Jan; Librizzi, Damiano; Bender, Lena; Jedelská, Jarmila; Yousefi, Behrooz H.; Schaefer, Jens et al. (2023): How to Xenograft Cancer Cells on the Chorioallantoic Membrane of a Fertilized Hen's Egg and Its Visualization by PET/CT and MRI. In: *ACS applied bio materials* 6(6), S. 2435–2445. DOI: 10.1021/acsabm.3c00237.
40. Shen, H-C Jennifer; He, Mei; Powell, Anathea; Adem, Asha; Lorang, Dominique; Heller, Charles et al. (2009): Recapitulation of pancreatic neuroendocrine tumors in human multiple endocrine neoplasia type I syndrome via Pdx1-directed inactivation of Men1. In: *Cancer research* 69(5), S. 1858–1866. DOI: 10.1158/0008-5472.CAN-08-3662.
41. Singh, Anukriti; Srivastava, Nidhi; Yadav, Anjali; Ateeq, Bushra (2020): Targeting AGTR1/NF-κB/CXCR4 axis by miR-155 attenuates oncogenesis in glioblastoma. In: *Neoplasia (New York, N.Y.)*

22 (10), S. 497–510. DOI: 10.1016/j.neo.2020.08.002.

42. Szaszák, Márta; Chen, Hung-Dar; Chen, Hao-Chia; Baukal, Albert; Hunyady, László; Catt, Kevin J. (2008): Identification of the invariant chain (CD74) as an angiotensin AGTR1-interacting protein. In: *The Journal of endocrinology* 199(2), S. 165–176. DOI: 10.1677/JOE-08-0190.
43. Tayler, Hannah M.; MacLachlan, Robert; Güzel, Özge; Fisher, Robert A.; Skrobot, Olivia A.; Abulfadl, Mohamed A. et al. (2024): Altered Gene Expression Within the Renin-Angiotensin System in Normal Aging and Dementia. In: *The journals of gerontology. Series A, Biological sciences and medical sciences* 79(1). DOI: 10.1093/gerona/glad241.
44. Tschanz, Fabienne; Bender, Sabine; Telarovic, Irma; Waller, Verena; Speck, Roberto F.; Pruschy, Martin (2021): The ADAM17-directed Inhibitory Antibody MEDI3622 Antagonizes Radiotherapy-induced VEGF Release and Sensitizes Non-Small Cell Lung Cancer for Radiotherapy. In: *Cancer research communications* 1(3), S. 164–177. DOI: 10.1158/2767-9764.CRC-21-0067.
45. Tu, Yuanbiao; Liu, Zicun; Wang, Fang; Liu, Peifei; Tao, Ji; Li, Changsheng et al. (2020a): AT1R-Specific Ligand Angiotensin II as a Novel SPECT Agent for Hepatocellular Carcinoma Diagnosis. In: *ACS sensors* 5(12), S. 4072–4080. DOI: 10.1021/acssensors.0c02180.
46. Tu, Yuanbiao; Tao, Ji; Wang, Fang; Liu, Peifei; Han, Zhihao; Li, Zhaolun et al. (2020b): A novel peptide targeting gastrin releasing peptide receptor for pancreatic neoplasm detection. In: *Biomaterials science* 8(9), S. 2682–2693. DOI: 10.1039/d0bm00162g.
47. Volonte, Daniela; Sedorovitz, Morgan; Cespedes, Victoria E.; Beecher, Maria L.; Galbiati, Ferruccio (2021): Cell autonomous angiotensin II signaling controls the pleiotropic functions of oncogenic K-Ras. In: *The Journal of biological chemistry* 296, S. 100242. DOI: 10.1074/jbc.RA120.015188.
48. Wagener, Nele; Buchholz, Malte; Bertolino, Philippe; Zhang, Chang X.; Di Fazio, Pietro (2022): Exploring the MEN1 dependent modulation of caspase 8 and caspase 3 in human pancreatic and murine embryo fibroblast cells. In: *Apoptosis: an international journal on programmed cell death* 27(1–2), S. 70–79. DOI: 10.1007/s10495-021-01700-1.
49. Zhang, Jun-Feng; Tao, Ling-Ye; Yang, Min-Wei; Xu, Da-Peng; Jiang, Shu-Heng; Fu, Xue-Liang et al. (2021): CD74 promotes perineural invasion of cancer cells and mediates neuroplasticity via the AKT/EGR-1/GDNF axis in pancreatic ductal adenocarcinoma. In: *Cancer letters* 508, S. 47–58. DOI: 10.1016/j.canlet.2021.03.016.
50. Zhou, Kuncheng; Li, Gang; Pan, Rongbin; Xin, Sulin; Wen, Weijie; Wang, Huiyi et al. (2024): Preclinical evaluation of AGTR1-Targeting molecular probe for colorectal cancer imaging in orthotopic and liver metastasis mouse models. In: *European journal of medicinal chemistry* 271, S. 116452. DOI: 10.1016/j.ejmech.2024.116452.

Figures

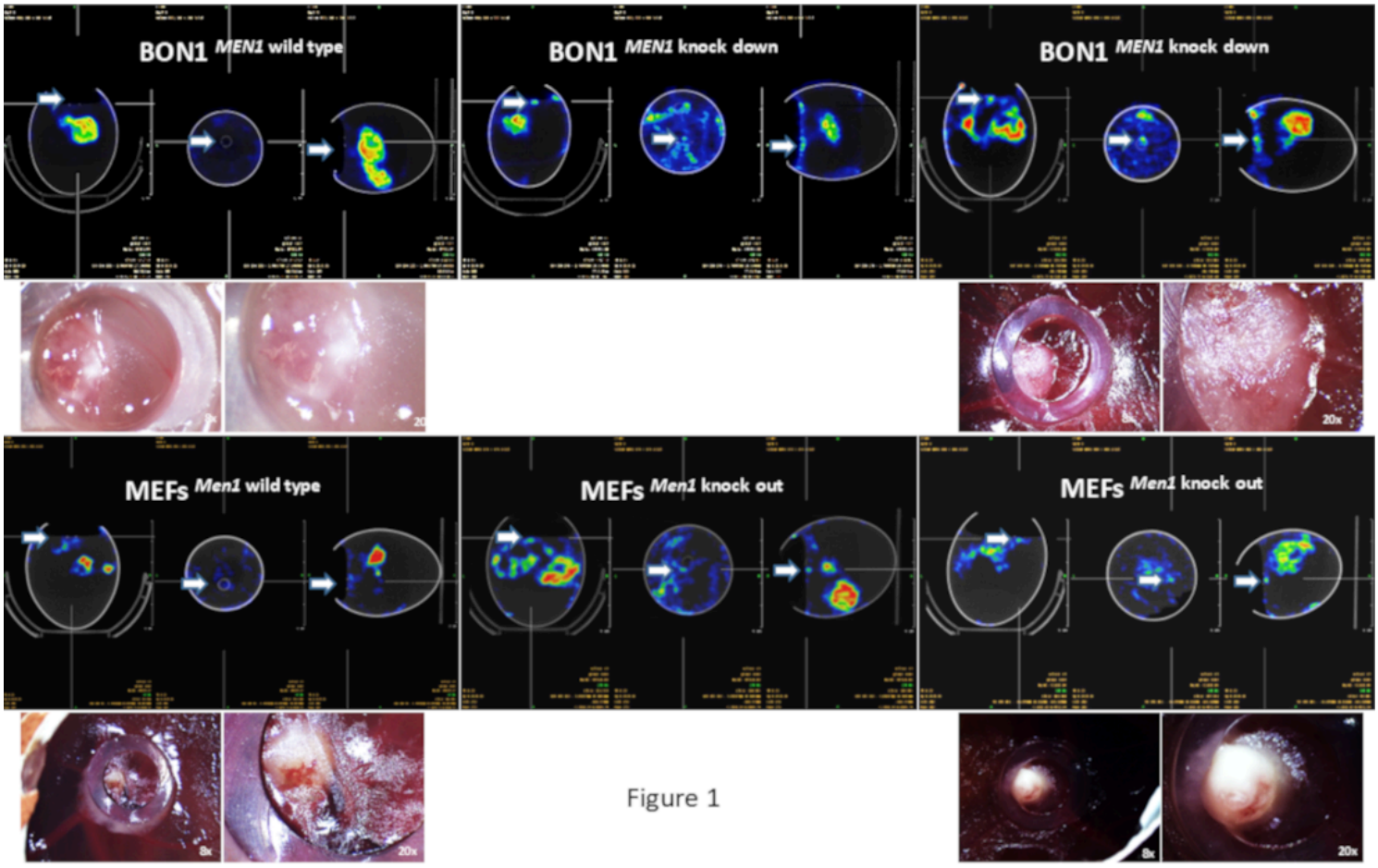

Figure 1

SPECT/CT of BON1 and MEFs CAM xenografts

Detection of angiotensin II radio tracer ([^{99m}Tc]-HYNIC-PEG4-Ang-II) in MEN1 wild type BON1, *MEN1* knocked down BON1, *Men1*$^{+/+}$ MEFs and *Men1*$^{-/-}$ MEFs. Below, stereomicroscopy micrographs of the xenografted cell derived mass. White arrows indicate the position of the xenografts in the CAM. Magnification of the stereomicrographs is 8X and 20X.

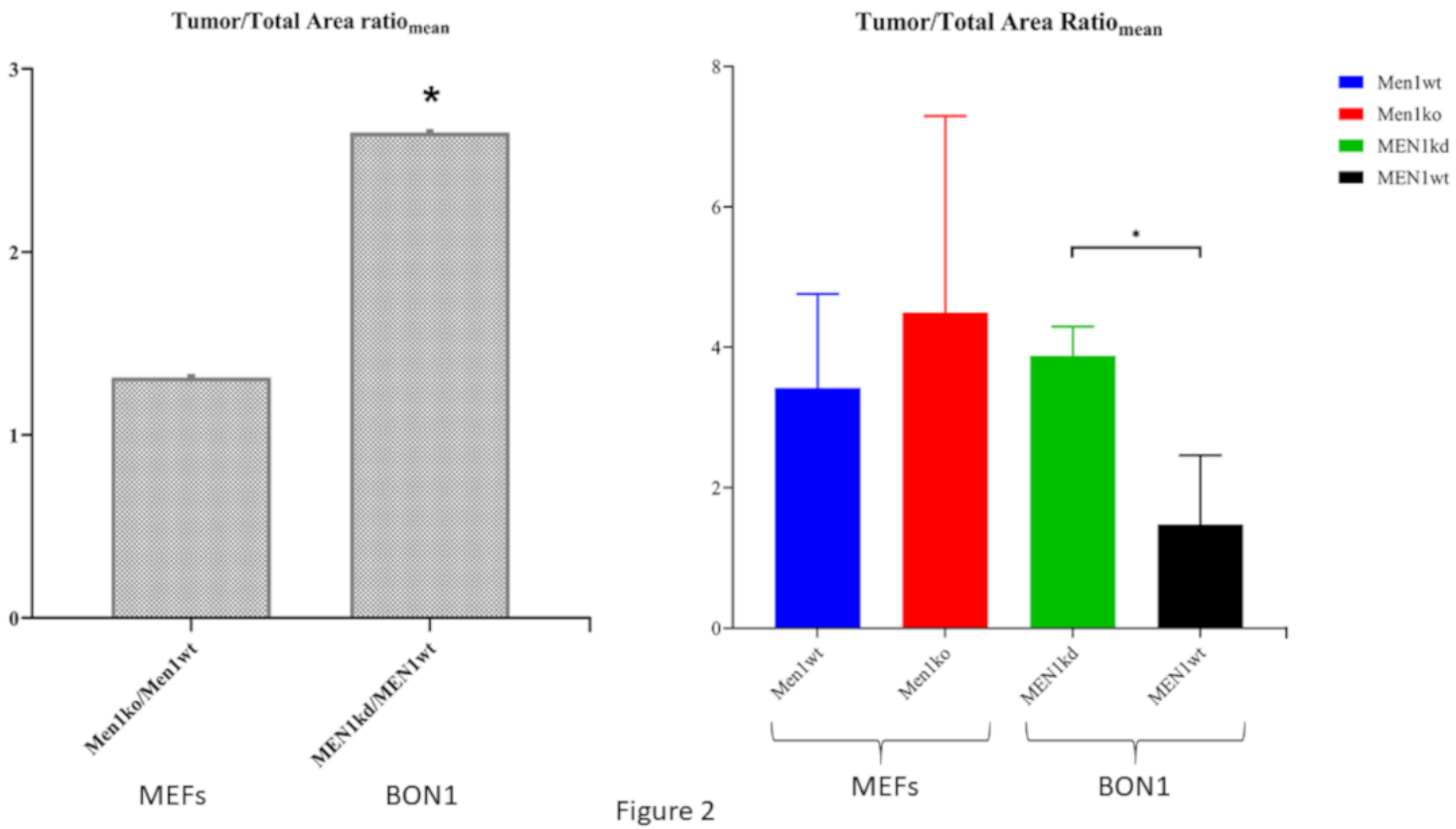

Figure 2

Quantification of the radio-labeled angiotensin II

The radioactivity of the radio tracer ([^{99m}Tc]-HYNIC-PEG4-Ang-II) was detected in the xenograft and in the chick body. Both signals were quantified and the signal of the chick body mass was subtracted as background. The graph on the left side highlights the quantification of the signal of *Men1*ko vs *Men1*wt (MEFs) and *MEN1*kd vs *MEN1*wt (BON1). The graph on the right side highlights the quantification of the signal of each single group. Here is shown the ratio of the radioactivity of the tumor mass vs the total area (chick embryo body mass) ± standard deviation. *p=0.0108 was statistically significant.

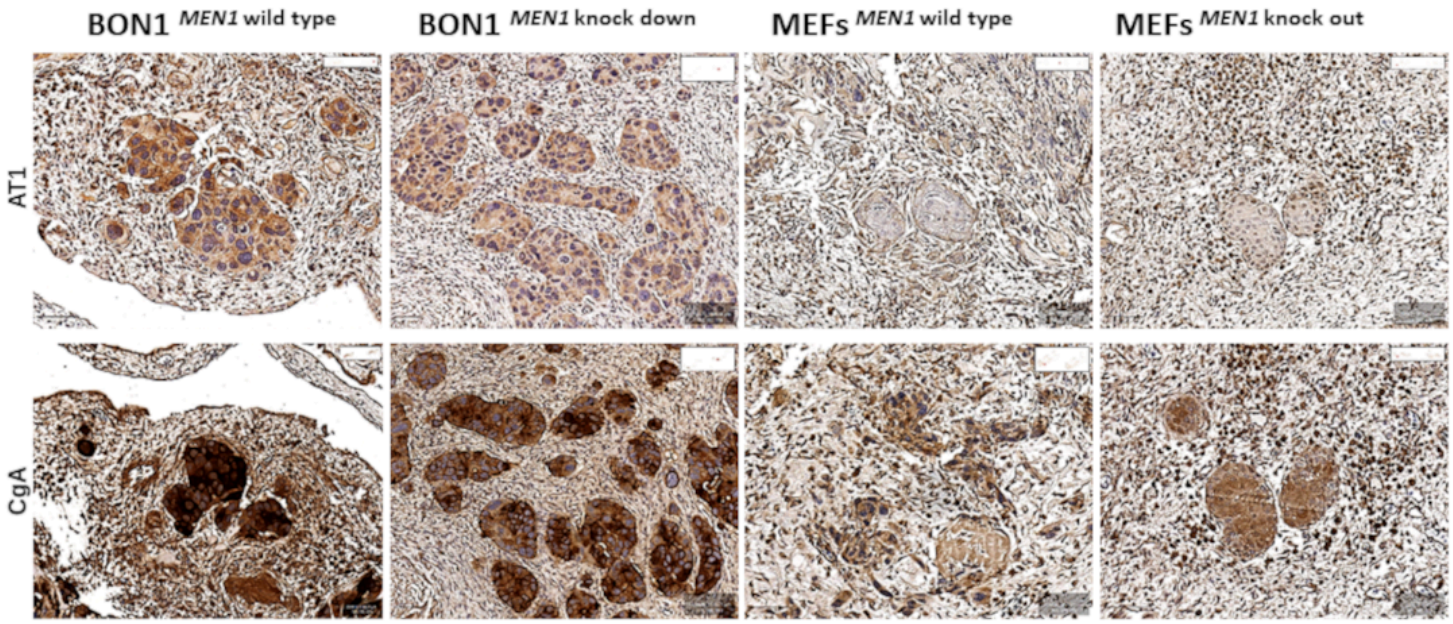

Figure 3

Detection of AT1 and CgA in BON1 and MEF CAM xenografts

Immunohistochemical detection of AT1 (upper micrographs) and CgA (lower micrographs) in *MEN1* wild type BON1, *MEN1* knocked down BON1, *Men1*$^{+/+}$ MEFs and *Men1*$^{-/-}$ MEFs. Magnification is 4X. Scalebar is 50 µm.

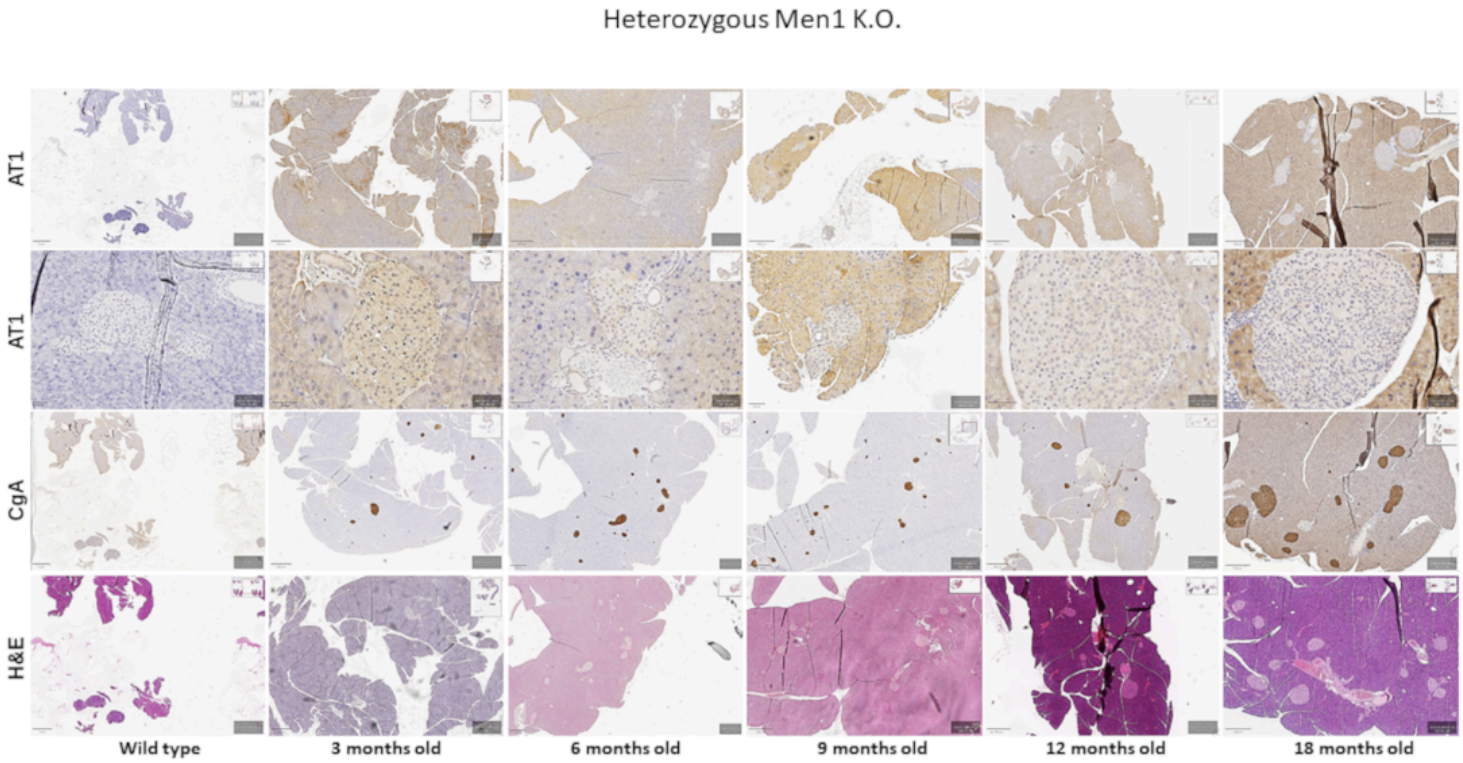

Figure 4

The proteins AT1 and CgA were immunohistochemically detected in the pancreatic tissue of heterozygouses *Men1*$^{flox/+}$ *Pdx*$^{Cre/Cre}$ mice. The pancreatic tissue was dissected from mice sacrificed at the age of 3, 6, 9, 12 and 18 months. *Men1* wild type mouse was stained for At1 and CgA as control. H&E staining was performed to confirm the tissue origin. Magnification is 4X. Scalebars are 50 and 400 µm.

Detection of AT1 and CgA in heterozygouses Men1 mice pancreatic tissue

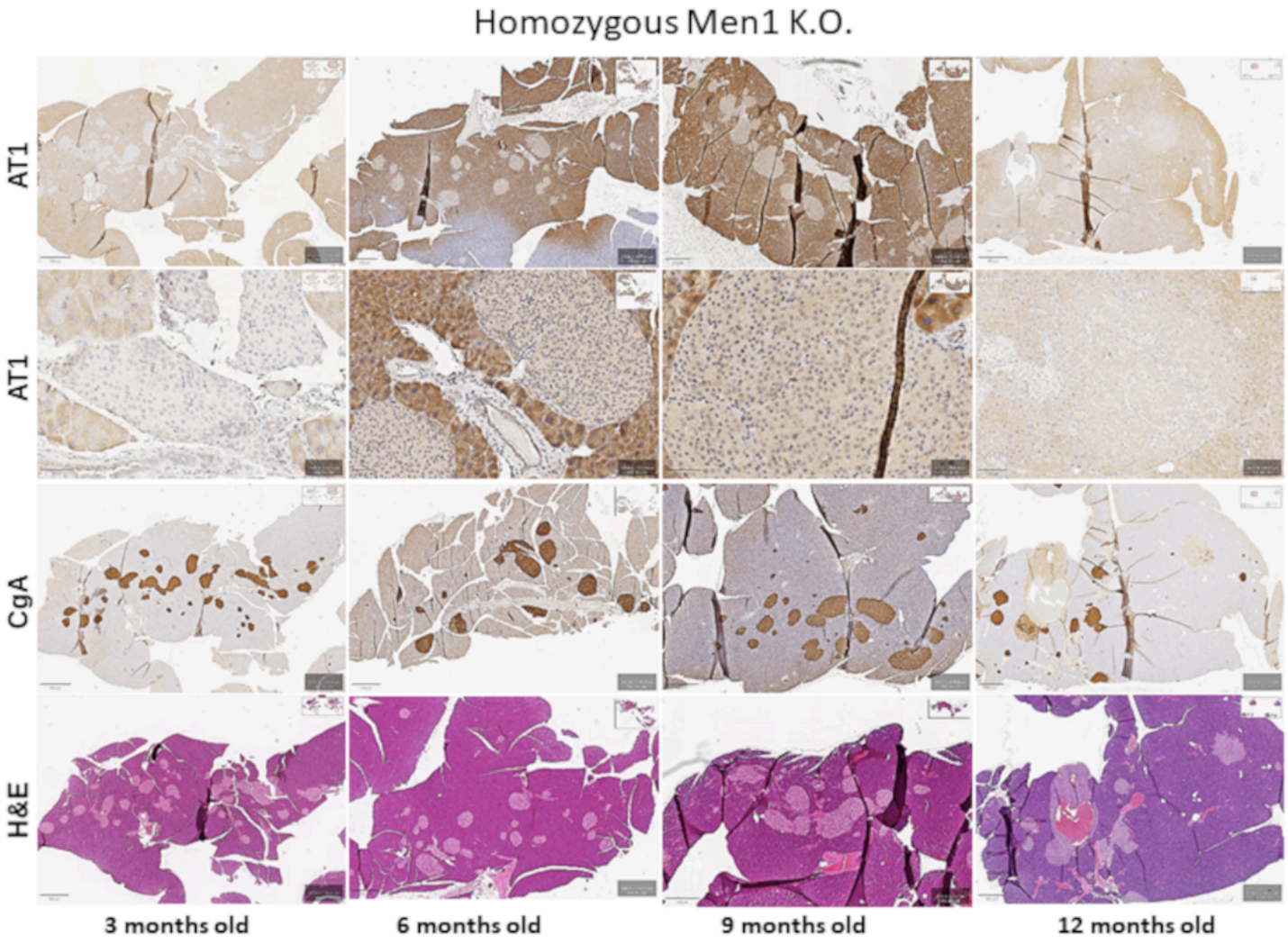

Figure 5

Detection of AT1 and CgA in homozygouses Men1 mice pancreatic tissue

The proteins AT1 and CgA were immunohistochemically detected in the pancreatic tissue of homozygouses *Men1*$^{flox/flox}$ *Pdx*$^{Cre/Cre}$ mice. The pancreatic tissue was dissected from mice sacrificed at the age of 3, 6, 9 and 12 months. H&E staining was performed to confirm the tissue origin. Magnification is 4X. Scalebars are 50 and 400 µm.

Supplementary Files

This is a list of supplementary files associated with this preprint. Click to download.

- Supplfiles.zip